

# UC Irvine

## UC Irvine Previously Published Works

### Title

Thermal, mechanical, optical, and morphologic changes in bovine nucleus pulposus induced by Nd:YAG ( $\lambda = 1.32 \mu\text{m}$ ) laser irradiation

### Permalink

<https://escholarship.org/uc/item/0cd2f0g6>

### Journal

Lasers in Surgery and Medicine, 28(3)

### ISSN

1050-9267

### Authors

Choi, Joon Y  
Tanenbaum, B Samuel  
Milner, Thomas E  
[et al.](#)

### Publication Date

2001

### DOI

10.1002/lsm.1046

### Copyright Information

This work is made available under the terms of a Creative Commons Attribution License, available at <https://creativecommons.org/licenses/by/4.0/>

Peer reviewed

# Thermal, Mechanical, Optical, and Morphologic Changes in Bovine Nucleus Pulposus Induced by Nd:YAG ( $\lambda = 1.32 \mu\text{m}$ ) Laser Irradiation

Joon Y. Choi, BA,<sup>1,2</sup> B. Samuel Tanenbaum, PhD,<sup>3</sup> Thomas E. Milner, PhD,<sup>4</sup> Xavier V. Dao,<sup>1</sup> J. Stuart Nelson, MD, PhD,<sup>1</sup> Emil N. Sobol, PhD,<sup>5</sup> and Brian J.F. Wong, MD<sup>1,6\*</sup>

<sup>1</sup>Beckman Laser Institute, University of California Irvine, Irvine, California 92612

<sup>2</sup>University of Rochester School of Medicine and Dentistry, Rochester, New York 14642

<sup>3</sup>Department of Engineering, Harvey Mudd College, Claremont, California 91711

<sup>4</sup>Biomedical Engineering Program, The University of Texas at Austin, Austin, Texas 78712-1084

<sup>5</sup>Center for Technological Lasers, Russian Academy of Sciences, Troitsk, Moscow Region, 142092 Russia

<sup>6</sup>Department of Otolaryngology-Head and Neck Surgery, University of California Irvine, Orange, California 92868

**Background and Objective:** To examine the biophysical effects of photothermal heating on herniated intervertebral discs during laser decompression surgery.

**Study Design/Materials and Methods:** Ex vivo bovine nucleus pulposus specimens were irradiated with a Nd:YAG laser ( $\lambda = 1.32 \mu\text{m}$ , 100 seconds exposure time, 9–31 W/cm<sup>2</sup>, 4.8 mm spot diameter), whereas changes in tissue thermal, mechanical, and optical properties were monitored by using, respectively, infrared radiometry, tissue tension measurements, and diffuse reflectance from a HeNe probe laser. Morphologic changes and mass reduction were monitored by recording shape changes on video and weighing specimens before and after laser exposure.

**Results:** At power densities below 20 W/cm<sup>2</sup>, evaporation of water and specimen volume reduction (shrinking) were consistently observed on video during irradiation. In contrast, above 20 W/cm<sup>2</sup>, vapor bubbles formed within the specimen matrix and subsequently ruptured (releasing heated vapors). When radiometric surface temperature approaches approximately 60 to 70°C (denaturation threshold for tissue), tissue tension begins to increase, which is consistent with observations of specimen length reduction. The onset of this change in tissue tension is also reflected in characteristic alterations in diffuse reflectance. With cessation of laser irradiation, a sustained increase in tissue tension is observed, which is consistent with changes in specimen length and volume. Higher laser power results in a faster heating rate and subsequently an accelerated tension change. Specimen mass reduction increased with irradiance from 19 to 72% of the initial mass for 9–31 W/cm<sup>2</sup>, respectively. Irradiated specimens did not return to their original shape after immersion in saline (48 hours) in contrast to air-dried specimens (24 hours), which returned to their original shape and size.

**Conclusion:** These observations suggest that photothermal heating results in irreversible matrix alteration causing shape change and volume reduction (observed on video and evidenced by the increase in tissue tension) taking place at approximately 65°C. Inasmuch as high laser power results in vapor bubble formation and speci-

men tearing, the heating process must be controlled. Diffuse reflectance measurements provide a noncontact, highly sensitive means to monitor dynamically changes in tension of nucleus pulposus. *Lasers Surg. Med.* 28:248–254, 2001. © 2001 Wiley-Liss, Inc.

**Key words:** cartilage; intervertebral disc; Nd:YAG laser; nucleus pulposus; spine surgery

## INTRODUCTION

The intervertebral disc is made up of fibrocartilage, which has properties similar to both hyaline cartilage and dense connective tissue [1]. The disc is heterogeneous consisting of a soft inner region (the nucleus pulposus, NP) surrounded by the annulus fibrosus (AF) composed of approximately 12 concentric lamellae [2]. The high osmolarity of the NP extracellular matrix results in swelling, which is limited by the surrounding AF and vertebral body end plates. As a result, this increased intradisc pressure balances axial load bearing forces [3]. In herniated disc syndrome, a structural defect in the AF results in partial extrusion of the NP, which may impinge on the adjacent nerve root, resulting in pain. The treatment of herniated disc requires decompression and evacuation of the NP, which can be accomplished by using laser irradiation at nonablative fluences to reduce the volume of the herniated segment.

Following the pioneering work by Ascher on percutaneous intradiscal laser nucleotomy [4], various laser procedures have been used for the treatment of herniated

Contract grant sponsor: Office of Naval Research; Contract grant number: N00014-94-0874; Contract grant sponsor: National Institutes of Health; Contract grant numbers: 1 K08 DC 00170-01, AR-43419, RR-01192, and HL-59472; Contract grant sponsor: The Whitaker Foundation; Contract grant number: WF-21025; Contract grant sponsor: Department of Energy; Contract grant number: 95-3800459.

\*Correspondence to: Brian J.F. Wong, MD, Beckman Laser Institute and Medical Clinic, University of California Irvine, 1002 Health Sciences Road East, Irvine, CA 92612.

E-mail: bjfwong@bli.uci.edu

Accepted 5 July 2000

discs [5–7]. Laser irradiation of the NP results in volume reduction readily observed by the naked eye. The success of minimally invasive laser disc procedures is well documented by several clinical studies [8–13]. Despite clinical implementation of laser-assisted disc operations, the mechanisms of action and biophysical changes in the NP accompanying laser irradiation have not been extensively studied, nor has feedback control been used to optimize this procedure.

The purpose of this study was to characterize the thermal, mechanical, optical, and morphologic changes in the NP during sustained Nd:YAG laser ( $\lambda = 1.32 \mu\text{m}$ ) irradiation. Volume changes were estimated by measuring changes in tissue tension (tensiometric force)  $T(t)$  in a rigidly secured specimen and mass loss (due to evaporation). These indirect methods were used as the irregular geometry and viscoelasticity of the NP preclude direct measurement. Morphologic changes were analyzed by using stop-action video imaging. Surface temperature of the NP specimen ( $S_c(t)$ ,  $^{\circ}\text{C}$ ) was estimated by measuring infrared emissions radiometrically. Structural alterations in the tissue matrix were indirectly monitored by measuring the changes in diffusely reflected light ( $I(t)$ ) from a second probe laser beam (HeNe,  $\lambda = 632.8 \text{ nm}$ ) during photothermal heating with the Nd:YAG laser. Finally, reversibility of the laser-mediated volume reduction was determined by observing shape and appearance changes in irradiated NP specimens after 48 hours of immersion in saline (in contrast to simply air-dried specimens).

## MATERIALS AND METHODS

Intervertebral discs were dissected from fresh bovine tails purchased at a local packing house. Bovine tails were chosen because of their large size, availability, and low cost. The NP was removed with a tissue punch (diameter = 8 mm). Specimens were immediately secured to the experimental apparatus (Fig. 1) to minimize water loss due to desiccation.

### Biophysical Measurements

Two straight-tip hemostat clamps secured the specimen to the experimental apparatus (Fig. 1). One hemostat was welded to a thin-beam load cell while the other was secured to a stationary ring-stand. A micropositioner attached to the load cell was used to adjust the initial tension across the stretched specimen. Laser irradiation resulted in specimen length reduction and an increase in  $T(t)$ .

NP specimens were irradiated for 100 seconds with the Nd:YAG laser ( $\lambda = 1.32 \mu\text{m}$ , 50 Hz PRR, Laser Aesthetics, Auburn, CA) at one of five power densities (9, 14, 20, 25, and  $31 \text{ W/cm}^2$ ). The laser energy was delivered by means of a 600- $\mu\text{m}$  core-diameter silica multimode optical fiber terminating in a collimating lens. Laser spot size (4.8 mm diameter) and power were measured with thermal paper and a pyroelectric meter (Model 10A-P, Ophir, Jerusalem, Israel), respectively.

Radiometric surface temperature ( $S_c(t)$ ,  $^{\circ}\text{C}$ ) was estimated by using a thermopile sensor (response time of 120 msec (95%), spectral sensitivity 7.6-18  $\mu\text{m}$ , Laser

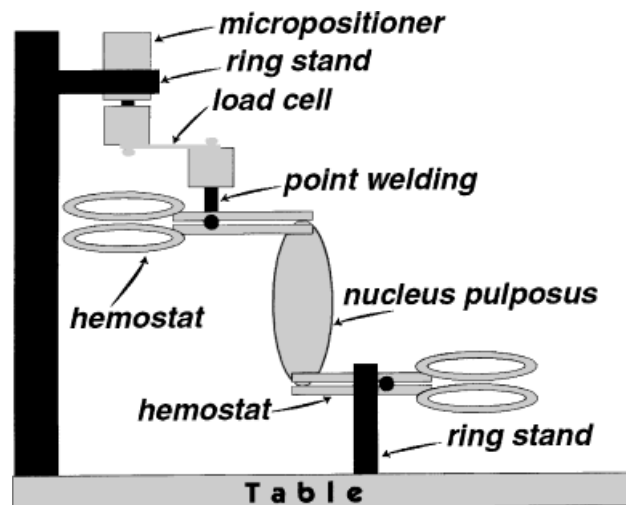


Fig. 1. Load-cell setup.

Aesthetics), and calibrated as previously described [14]. Two load cells with different peak capacities (LCL-454G (454 g) and LCL-005 (2.27 kg), Omega Engineering, Inc., Stamford, CT) were used to measure tissue tension ( $T(t)$ ). The signals from these load cells were amplified and low-pass filtered (3 db cutoff at 30Hz) with a low-noise preamplifier (model SRS 560, Stanford Research Systems, Sunnyvale, CA). Diffusely reflected light from the HeNe probe laser ( $\lambda = 632.8 \text{ nm}$ , 15 mW, Melles Griot) incident on the nonirradiated surface of the specimen was collected in an integrating sphere and measured with a silicon photodetector (model 2001, New Focus, Mountain View, CA) to yield  $I(t)$ . HeNe laser intensity was amplitude-modulated (900 Hz) with a mechanical chopper (model R540, Stanford Research Systems) and synchronously detected with a lock-in amplifier ( $\tau = 30 \text{ msec}$ , model SR830, Stanford Research Systems). An analog to digital converter (AT-MIO-16XE-50, National Instruments, Austin, TX) was used to record  $S_c(t)$ ,  $I(t)$ , and  $T(t)$  by using software written in Labview (National Instruments) running on a PC.  $I(t)$  and  $T(t)$  were normalized to arbitrary units (a.u.).

During laser irradiation, NP specimens maintained under tension undergo readily observed changes in morphology. A wide-angle endoscope (30 degrees, 26033 BP, Karl Storz, Culver City, CA) and CCD camera (Endocam 202101 20, Karl Storz) illuminated with a Xenon light source (Karl Storz) were used to record images at video rate. A short wavelength pass optical filter (600 nm, Corion, Franklin, MA) placed in front of the endoscope eliminated detection of scattered light from the HeNe probe laser in recorded video images.

The experimental setup is illustrated in Figure 2. The load cell and specimen were positioned close to the integrating sphere to optimize collection efficiency of diffusely reflected light from the HeNe probe laser. Evaporative water losses after laser irradiation were measured by weighing specimens immediately before and after 100

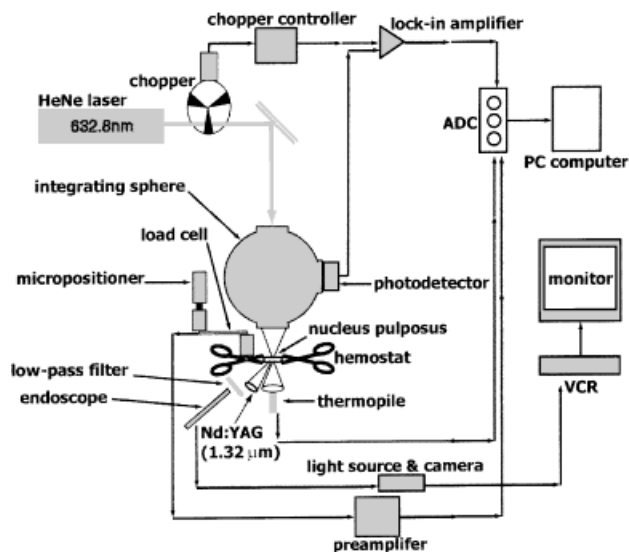


Fig. 2. Schematic of experimental setup.

seconds of irradiation at five different power densities (9, 14, 20, 25, and 31 W/cm<sup>2</sup>). Mass loss due to evaporation (without laser irradiation) over the 100-second time interval was negligible. Percent change in mass ( $[\text{mass before} - \text{mass after irradiation}] / \text{mass before irradiation} \times 100\%$ ) was calculated.

Control (nonirradiated) tissue specimens were allowed to dry at ambient temperature for 24 hours. To evaluate reversibility of laser induced volume reduction, NP speci-

mens of identical size and mass were irradiated for 100 seconds by using the same power densities as above, and then immediately immersed in saline solution for 48 hours. After immersion in saline, both treatment and control specimens were removed and compared in terms of morphology, volume, and texture.

## RESULTS

A sequence of video images of an NP irradiated at 20 W/cm<sup>2</sup> (Fig. 3) illustrates the dynamic shape changes as well as volume reduction accompanying laser irradiation. Before irradiation, the specimen is opaque and moist (Fig. 3a), with a thickness of approximately 5 mm. Morphologic changes begin a few seconds after the onset of the irradiation and proceed gradually. At 30 seconds after laser irradiation, the upper two thirds of the specimen starts to warp and shift in position as volume reduction begins (Fig. 3b) and the distance between the two hemostats shortens. At 60 seconds after laser irradiation, length and volume reduction continues (Fig. 3c). After termination of laser irradiation, the specimen has a smaller volume (Fig. 3d) indicated by shorter vertical length and thickness (3 mm). The tissue has a more translucent, yellowish hue and desiccated texture.

At higher power, a "popping" phenomenon is observed (31 W/cm<sup>2</sup>, Fig. 4). Figure 4a shows the specimen before irradiation. After 28 seconds of laser exposure, expansion of the NP on the nonirradiated surface together with what seems to be bubble formation within the tissue matrix as indicated by the arrow (Fig. 4b). Two seconds later (Fig. 4c), this bubble bursts, resulting in a loud popping

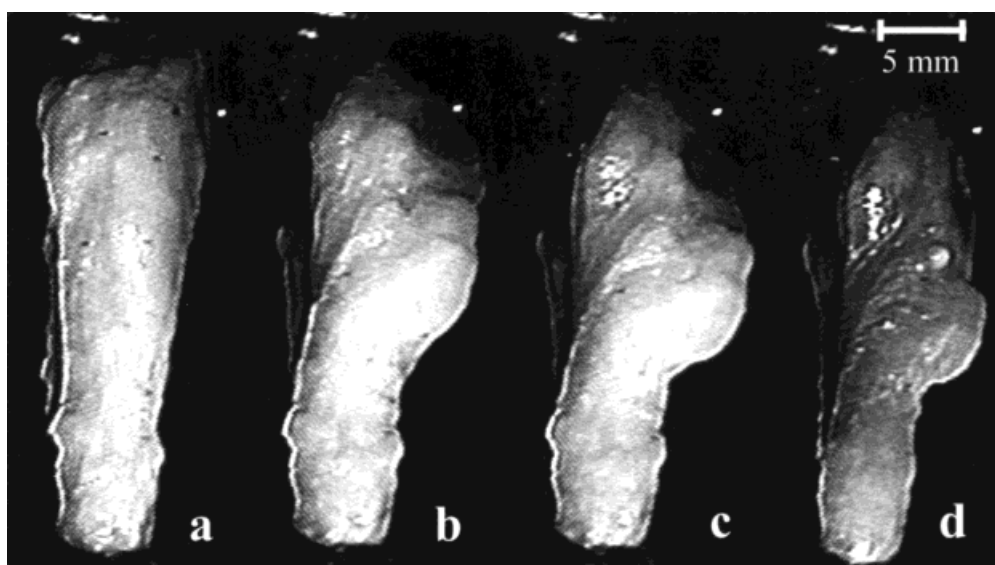


Fig. 3. Montage of stop-action video images at 20 W/cm<sup>2</sup>. **a:** At 0 seconds, the initial morphology of the specimen before irradiation is shown. **b:** After 30 seconds of irradiation, the gradual shape changes along with a slight decrease in specimen length indicated by the distance between the two

hemostats. **c:** At 60 seconds, further changes in shape and volume as irradiation continues. **d:** At 100 seconds, specimen volume decreased, as indicated by shorter vertical length and thickness (5 mm in frame a to 3 mm in frame d).

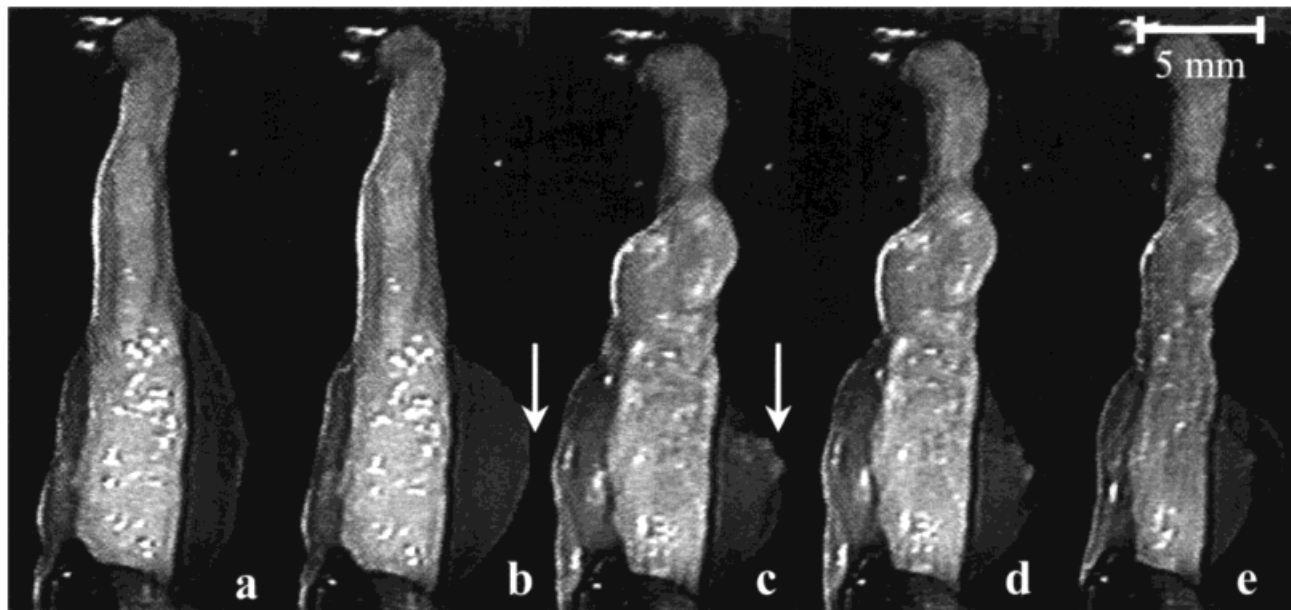


Fig. 4. Montage of stop-action video images at  $31 \text{ W/cm}^2$ . **a:** At 0 seconds, the initial morphology before irradiation is shown. **b:** At 28 seconds, the expanding bubble is indicated by the big arrow. **c:** At 30 seconds, the bubble bursts, releasing hot vapor

through the opening. **d:** At 33 seconds, the bubble deflates after bursting. **e:** At 40 seconds, the deflated bubble and overall specimen thickness decrease from 5 mm in a to 3 mm in e.

noise and the release of water vapor. The rupture or “popping” can be observed in the third frame as indicated by the arrow. Three seconds after the popping (Fig. 4d), the bubble gradually deflates as the vapor continues to escape through the ruptured opening. Seven seconds after the popping (Fig. 4e), the bubble volume appears further reduced. Between Figure 4a and e, the specimen thickness has reduced from 5 to 3 mm.

Figure 5 depicts changes in  $S_c(t)$ ,  $T(t)$ , and  $I(t)$  during laser irradiation for 100 seconds ( $14 \text{ W/cm}^2$ ).  $S_c(t)$  initially increases at the onset of the irradiation with a high heating rate ( $d(S_c(t))/dt \sim 5^\circ\text{C}/\text{sec}$ ). This heating rate gradually decreases until the temperature stabilizes and plateaus (steady state) after 18 seconds. Both  $d(S_c(t))/dt$  and steady state plateau temperature increase with higher power density.  $T(t)$  begins to increase when  $S_c(t)$  reaches  $63.4^\circ\text{C}$  (at 11 seconds). At this same time,  $I(t)$  increases, peaks, and decreases (despite sustained irradiation). Inasmuch as the observed peak in  $I(t)$  is coincident with the onset of increase in tissue tension, this noncontact optical measurement may be used to monitor dynamic changes in NP mechanical properties. With termination of laser irradiation,  $S_c(t)$  cools to ambient temperature and  $T(t)$  decreases from the peak down to a new equilibrium value (higher than the initial baseline). This sustained increase in tissue tension is observed and is consistent with specimen shortening, volume reduction, and mass loss.

Multiple peaks in the light scattering ( $I(t)$ ) curves are occasionally observed (particularly at higher power) and coincide with abrupt shape or position changes in the specimen caused by tearing or rotation. When multiple

peaks are observed as in Figure 6, the first peak correlates with the previously described changes in  $S_c(t)$  and  $T(t)$ . The “popping” phenomenon accompanying high power irradiation (illustrated in Fig. 4) is accompanied by discontinuities in  $S_c(t)$ ,  $T(t)$  and  $I(t)$ . At popping,  $S_c(t)$  abruptly falls from  $111^\circ\text{C}$  to  $93^\circ\text{C}$  as hot vapor rapidly escapes through the opening on the surface, and then  $S_c(t)$  starts to increase again as irradiation continues.  $T(t)$  falls abruptly and then slowly increases in the same manner as  $S_c(t)$  as the released vapor suddenly relieves the pressure within the bubble and relaxes the specimen momentarily.  $I(t)$ , on the other hand, suddenly increases past its initial starting point as the popping creates rapid shifts in position.  $I(t)$  resumes its descent again once the specimen becomes stable.

Before irradiation or air-drying (at ambient temperature), both treatment and control specimens are soft and opaque. After irradiation, focal volume reduction in the laser target site is observed and the irradiated regions on the surface feel stiffer and brittle and appear more translucent and yellow than the nonirradiated areas. Irradiation also causes “dimpling” of the NP, which results in the creation of a biconcave disc as the nonirradiated peripheral regions of the NP retain all their initial characteristics; the degree of dimple formation increases with increasing power density. Nonirradiated specimens allowed to dry at ambient temperatures for 24 hours show uniform volume reduction and yellowish discoloration with a brittle, desiccated texture throughout, but return to their native appearance and texture after immersion in saline (48 hours). When laser irradiated specimens are

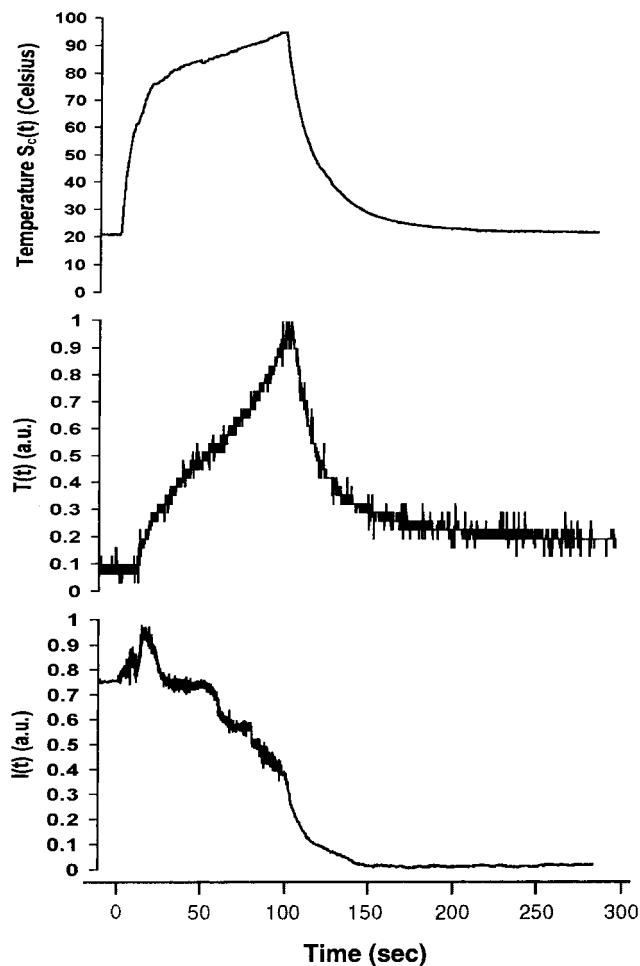


Fig. 5. Simultaneous measurements of  $S_c(t)$ ,  $I(t)$ , and  $T(t)$  at  $14 \text{ W/cm}^2$  by using 454-g cell. Note the temporal coincidence of the first (if there is more than one) peak in  $I(t)$  with the beginning of the rise in  $T(t)$ . This peak in  $I(t)$  also corresponds to  $S_c(t)$  of  $60\text{--}70^\circ\text{C}$ . The steady-state surface temperature at the plateau increases with increasing power density.  $I(t)$  and  $T(t)$  are adjusted to values between 0 and 1, and the units are labeled as arbitrary units (a.u.).

immersed in saline for 48 hours, the changes in the laser-irradiated regions are still readily apparent while non-irradiated regions (and all control specimens) return to their initial shape, color, and texture. Changes in specimen mass after laser irradiation (Fig. 7) support these findings. Figure 7 also shows that the amount of mass change upon irradiation is directly proportional to power density. Air-dried specimens (ambient temperature, 100 seconds) show a small reduction in mass of 3.6%.

## DISCUSSION

In this study, we attempted to characterize various biophysical changes in the NP accompanying laser-mediated volume reduction. Indirect methods for measuring volume changes were used, because the irregular shape and viscoelasticity of the NP do not allow direct measurement

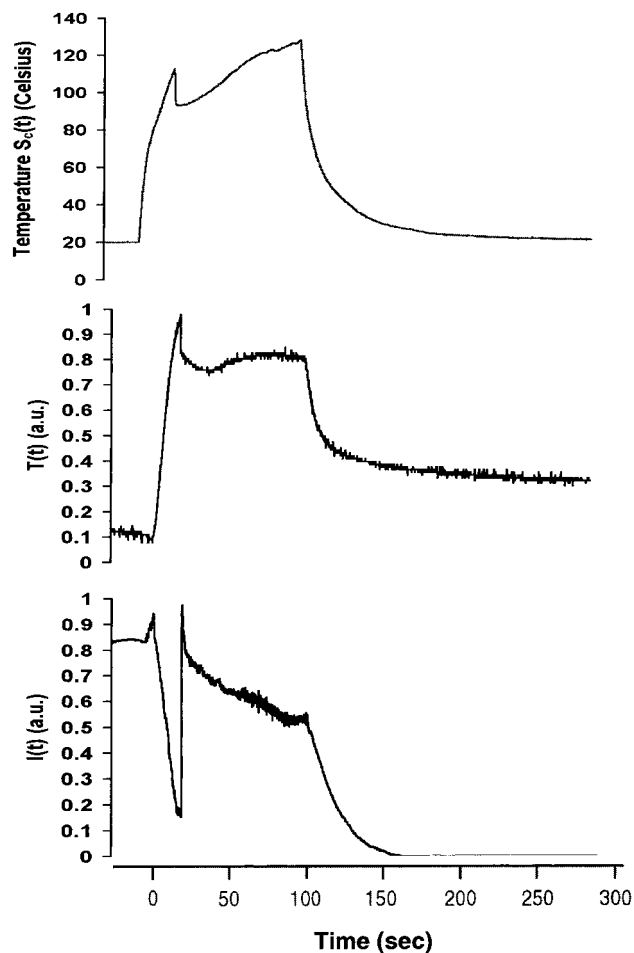


Fig. 6. Simultaneous measurements of  $S_c(t)$ ,  $I(t)$ , and  $T(t)$  at  $31 \text{ W/cm}^2$  by using 2.27-kg cell. Note the discontinuities in  $S_c(t)$ ,  $I(t)$ , and  $T(t)$  reflecting the popping of vapor bubbles.  $I(t)$  and  $T(t)$  are adjusted to values between 0 and 1, and the units are labeled as arbitrary units (a.u.).

techniques, and the high water absorbent nature precludes the use of techniques based on Archimedes' principle. Hence, we measured tissue tension  $T(t)$ , which increases with reduction in specimen length and volume and correlates with observed morphologic changes recorded on video. The mass reduction measurements demonstrate that specimen volume decreases with increasing incident laser power density as observed in clinical studies [15,16]. Both evaporation of water and NP matrix denaturation contribute to specimen volume reduction. Inasmuch as laser-irradiated specimens did not return to their original shape, texture, or appearance after rehydration (48 hours), the volume reduction process seems irreversible and dominated by the denaturation of tissue matrix proteins.

$S_c(t)$  and  $I(t)$  measurements provide additional insight into the nature of laser-mediated volume reduction. The presence of a phase transition is suggested by the observation of a peak in  $I(t)$  corresponding to surface temperature of approximately  $60$  to  $70^\circ\text{C}$  and the onset of increased

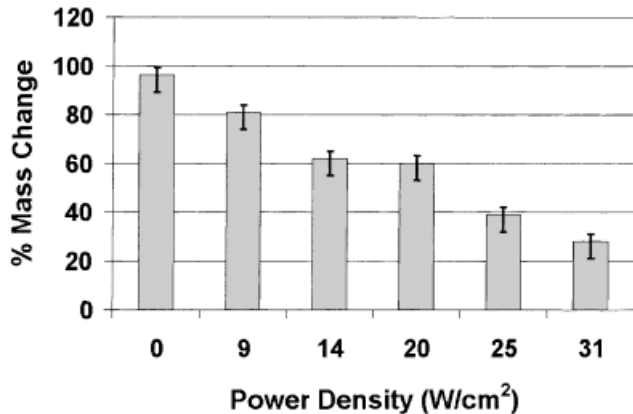


Fig. 7. Mass reduction study results; the amount of mass change upon irradiation seems to be directly proportional to power density. The percentage of initial mass was plotted for each power density after irradiating each specimen for 100 seconds. Controls were air-dried at ambient temperature for 100 seconds before weighing.

tissue tension ( $T(t)$ ). This finding is similar to observations of temperature-dependent stress relaxation in septal cartilage tissues during laser-mediated cartilage reshaping [17].

Shape and volume changes in NP specimens vary dramatically depending on the laser irradiations as illustrated in Figures 3 and 4, and the accompanying tension changes occur over a wide dynamic range. Hence, two load cells with different sensitivities (maximum load 454 g and 2.27 kg) were used for the measurement of small and large changes in tension, which correspond to low and high power laser irradiation, respectively. A 454-g load cell was adequate for a power density up to 14 W/cm<sup>2</sup>, but the “popping” phenomenon at 31 W/cm<sup>2</sup> created a tension change that went beyond the capacity of the 454-g cell. Therefore, a 2.27-kg cell was used for the high power experiments involving the “popping” phenomenon.

Motion artifacts accompanying abrupt shape changes are responsible for the observation of multiple peaks in  $I(t)$ . Nonuniformity of specimen shape and size along with localized heating create unpredictable patterns of volume reduction in NP. Shearing force from rapid increases in tension can cause tearing or stretching of thinner parts of NP resulting in abrupt specimen movement and the observation of multiple points of peaks in  $I(t)$  and  $T(t)$  (Fig. 6). “Popping” phenomenon (illustrated in Fig. 4) is the most extreme illustration of this change and results in discontinuities in  $S_c(t)$ ,  $T(t)$ , and  $I(t)$  as illustrated in Figure 6 with power density at 31 W/cm<sup>2</sup>. As water vapor is observed escaping from a “burst” bubble within the tissue matrix, the sudden decrease in temperature accompanying the rupture likely results from the loss of heated vapor. Tension decreases as noted by the abrupt decrease in  $T(t)$  (Fig. 6). At power densities below 20 W/cm<sup>2</sup>, bubble

formation is rarely observed, and all three variables show continuous behavior. Still, a constant thin stream of evaporating water is observed throughout the irradiation (although not captured in any of the still images in Figs. 3 and 4), thereby underscoring the role of vaporization in the laser-mediated volume reduction of nucleus pulposus. Clinically, the popping phenomenon is undesirable. Crucial structures (e.g. nerve roots and spinal cord) in proximity to the herniated NP may be injured by the sudden release of the hot vapor. Therefore, it is critical that tissue properties and laser power be dynamically monitored to minimize possible injury.

Other reported complications of laser nucleotomy include damage to the end plates between nucleus pulposus and adjacent vertebral bodies, although the long-term effects are not known [18]. Still, the thermal damage beyond the target area may be minimized by controlling the size of the primary zone of optical energy deposition, so-called “optical zone,” and the laser irradiation time [19]. The application of cryogen spray cooling is another possible method to avoid potential injury while allowing rapid delivery of laser energy [20]. Use of diffuse reflectance and surface temperature measurements as the feedback control parameters could also minimize injury because they closely reflect undergoing structural changes in the irradiated tissue [21].

Temperature feedback control systems are already available. For example, the temperature of the laser-irradiated tissues can be remotely sensed by an infrared fiber optic radiometer, which, in turn, controls the irradiation power [22]. Using a temperature probing tip inserted in the target tissue is another effective method of feedback temperature control [23]. In light of these advances, the incorporation of the diffuse reflectance into the feedback control system could be achieved by adding an anterograde fiber carrying probe light to the target and a retrograde fiber transmitting reflected light back to the detector. The temperature feedback system is commercially available (i.e., SpineCath, Oraflex ElectroThermal Probe, ORA-50 S Spine Generator, Oratec, Menlo Park, CA), but the diffuse reflectance has not been implemented as a laser feedback control parameter, to our knowledge.

The advantage of laser treatment over the conventional open discectomy is compelling, because it is done by means of a minimally invasive technique that offers quicker recovery and equivalent long-term results. It could be performed percutaneously by means of a catheter by using a guiding fluoroscope or possibly even an endoscope. Quicker recovery means a shorter hospital stay; therefore, the laser treatment also decreases health care costs. Recently, the radiofrequency (RF) technique has gained acceptance as another minimally invasive modality for treating herniated discs. Whether or not one modality is more effective than the other remains to be seen. However, one clear advantage of a laser over RF is that it is a noncontact modality, whereas RF requires insertion of the electrodes into the target tissue. Furthermore, costs of lasers are decreasing dramatically and, thus, should compete with the RF modality at some point in the future.

## CONCLUSIONS

This study demonstrates that photothermal heating results in localized irreversible volume reduction in nucleus pulposus. Characteristic changes in thermal, optical, and mechanical properties reflect the underlying modifications in the NP matrix and suggest denaturation as the major underlying mechanism. Light scattering measurements can be used as a temporal cue to indicate the beginning of matrix alterations occurring in the NP. Power densities greater than 20 W/cm<sup>2</sup> may cause interstitial vapor bubble formation, resulting in the release of heated water vapor. In turn, this may result in thermal injury to adjacent neural structures. Infrared radiometric surface temperature and light scattering measurements may provide a cost-effective means to monitor tissue property changes, control heating, and improve the safety of this procedure.

## REFERENCES

- Ross MH, Romrell LJ, Kaye GI, Cartilage. In: *Histology a text and atlas*. Baltimore: Williams & Wilkins 1995. p 132–149.
- Ghosh P. *The Biology of the intervertebral disc*. Boca Raton, FL: CRC Press, Inc; p 2–33.
- Iatridis JC, Weidenbaum M, Setton LA, Mow VC. Is the nucleus pulposus a solid or a fluid? Mechanical behaviors of the nucleus pulposus of the human intervertebral disc. *Spine* 1996;21:1174–1184.
- Ascher PW. Application of the laser in neurosurgery. *Lasers Surg Med* 1986;2:91–97.
- Helidonis E, Volitakis M, Naumidi I, Velegrakis G, Bizakis J, Christodoulou P. The history of laser thermo-chondro-plasty. *Am J Otolaryngol* 1994;15:423–428.
- Yonezawa T, Tanaka S, Watanabe H, Onomura T, Atsumi K. Percutaneous intradiscal laser discectomy. In: Mayer HM, Brock M, editors. *Percutaneous lumbar discectomy*. Berlin: Springer-Verlag; 1989. p 197–204.
- Choy DSJ, Case RB, Fielding W. Percutaneous laser nucleolysis of lumbar disc. *N Engl J Med* 1987;317:771–772.
- Bosacco SJ, Bosacco DN, Berman AT, Cordover A, Levenberg RJ, Stellabotte J. Functional results of percutaneous laser discectomy. *Am J Orthop* 1996;825–828.
- Choy DSJ. Percutaneous Laser Disc Decompression (PLDD): a new treatment modality for herniated discs. *Lasers Surg Med* 1998;(Suppl 10):66.
- Casper GD, Hartman VL, Mullins L. Results of a clinical trial of the Holmium:YAG laser in disc decompression utilizing a side-firing fiber: a two-year follow-up. *Lasers Surg Med* 1996;19:90–96.
- Choy DSJ. Percutaneous Laser Disc Decompression (PLDD): 352 cases with an 8.5 year follow-up. *J Clin Laser Med Surg* 1995;13:17–21.
- Sherk HH, Black JD, Prodoehl JA, Cummings RS. Laser discectomy. *Orthopaedics* 1993;16:573–576.
- Chiu JC, Clifford T, Greenspan M, Negron F, Princenthal RA, Carter J. Holmium laser (at non-ablative low energy level) thermodiskoplasty through disk shrinkage with tightening effect. *Lasers Surg Med* 1998;(Suppl 10):14–15.
- Anvari B, Milner TE, Tanenbaum BS, Kimel S, Svaasand LO, Nelson JS. Selective cooling of biological tissues: application for thermally mediated therapeutic procedures. *Phys Med Biol* 1995;40:247–252.
- Min K, Leu H, Zweifel K. Quantitative determination of ablation in weight of lumbar intervertebral discs with holmium:YAG laser. *Lasers Surg Med* 1996;18:187–190.
- Buchelt M, Schlangmann B, Schmolke S, Siebert W. High power Ho:YAG laser ablation of intervertebral discs: effects on ablation rates and temperature profile. *Lasers Surg Med* 1995;16:179–183.
- Sobol E, Kitai M, Jones N, Sviridov A, Milner T, Wong B. Heating and structural alterations in cartilage under laser radiation. *IEEE J Quant Elect* 1999;35:532–539.
- Nerubay J, Caspi I, Levinkopf M, Tadmor A, Bubis J. Percutaneous laser nucleolysis of the intervertebral lumbar disc. *Clin Orthop Relat Res* 1997;337:42–44.
- Jacques SL. Role of tissue optics and pulse duration on tissue effects during high-power laser irradiation. *Appl Optics* 1993;32:2447–2454.
- Anvari B, Tanenbaum BS, Milner TE, et al. Spatially selective photocoagulation of biological tissues: feasibility study utilizing cryogen spray cooling. *Appl Optics* 1996;35:3314–3320.
- Wong B, Milner TE, Anvari B, Sviridov A, Omelchenko A, Bagratashvili VV, Sobol E, Nelson JS. Measurement of radiometric surface temperature and integrated backscattered light intensity during feedback-controlled laser-assisted cartilage reshaping. *Lasers Med Sci* 1998;14:66–72.
- Shenfeld O, Ophir E, Goldwasser B, Katzir A. Silver halide fiber optic radiometric temperature measurement and control of CO<sub>2</sub> laser-irradiated tissues and application to tissue welding. *Lasers Surg Med* 1994;14:323–328.
- Ivarsson K, Olsrud J, Stureson C, Möller PH, Persson BR, Tranberg K. Feedback interstitial diode laser (805 nm) thermotherapy system: ex vivo evaluation and mathematical modeling with one and four-fibers. *Lasers Surg Med* 1998;22:86–96.